



Published in final edited form as:

Sci Transl Med. 2017 November 29; 9(418): . doi:10.1126/scitranslmed.aam6375.

Rescue of Pompe disease in mice by AAV-mediated liver delivery of secretable acid α -glucosidase

Francesco Puzzo^{1,2,*}, Pasqualina Colella^{1,*}, Maria G. Biferi³, Deeksha Bali⁴, Nicole K. Paulk⁵, Patrice Vidal^{1,3}, Fanny Collaud¹, Marcelo Simon-Sola^{1,3}, Severine Charles¹, Romain Haret³, Christian Leborgne¹, Amine Meliani^{1,3}, Mathilde Cohen-Tannoudji³, Stephanie Astord³, Bernard Gjata¹, Pauline Sellier^{1,3}, Laetitia van Wittenberghe¹, Alban Vignaud¹, Florence Boisgerault¹, Martine Barkats³, Pascal Laforet⁶, Mark A. Kay⁵, Dwight D. Koeberl⁷, Giuseppe Ronzitti^{1,†}, and Federico Mingozzi^{1,3,†}

¹INTEGRARE, Genethon, Inserm, Univ Evry, Université Paris-Saclay, 91002 Evry, France

²Department of Life Sciences and Biotechnology, University of Ferrara, Ferrara, Italy

³University Pierre and Marie Curie Paris 6 and INSERM U974, Paris, France

†Corresponding author: gronzitti@genethon.fr (G.R.); fmingozzi@genethon.fr (F.M.).

*These authors contributed equally to this work.

SUPPLEMENTARY MATERIALS

www.sciencetranslationalmedicine.org/cgi/content/full/9/418/eaam6375/DC1

Materials and Methods

Fig. S1. Human *GAA* transgene engineering.

Fig. S2. Selection of engineered human *GAA* transgenes in vitro and in vivo.

Fig. S3. *GAA* activity and liver vector transduction in vivo.

Fig. S4. Histological evaluation of heart, diaphragm, and quadriceps of treated *Gaa*^{-/-} mice and controls.

Fig. S5. *GAA* uptake and autophagic buildup in quadriceps of Pompe mice.

Fig. S6. Quantification of lysosomal *GAA* in brain of mouse model of Pompe disease.

Fig. S7. Anti-human *GAA* transgene humoral immune responses in *Gaa*^{-/-} mice.

Fig. S8. Weight of treated *Gaa*^{-/-} mice and controls.

Fig. S9. Baseline measurements in *Gaa*^{-/-} mice and controls.

Fig. S10. Long-term outcome of gene therapy in treated *Gaa*^{-/-} mice and controls.

Fig. S11. Liver transduction of NHPs treated with AAV8 encoding for the engineered sp7-8-co*GAA* transgene.

Table S1. *GAA* activity and glycogen content in Pompe mice 3 months after treatment at a vector dose of 5×10^{11} vg/kg.

Table S2. *GAA* activity and glycogen content in Pompe mice 3 months after treatment at a vector dose of 2×10^{12} vg/kg.

Table S3. *GAA* activity and glycogen content in Pompe mice 10 months after treatment at a vector dose of 2×10^{12} vg/kg.

Table S4. Long-term outcome of respiratory functions after gene therapy in treated *Gaa*^{-/-} mice and controls.

References (65–69)

Author contributions: F.P., P.C., G.R., and F.M. directed the study and wrote the manuscript. F.P., P.C., and G.R. performed most of the experiments and data analysis. F.P., P.C., M.G.B., P.L., G.R., and F.M. contributed to the interpretation of results and provided critical insights into the significance of the work. M.B., M.G.B., M.C.-T., and S.A. performed the analyses of mouse spinal cord. N.K.P. and M.A.K. generated the engineered AAV vector serotypes tested in primary hepatocytes. D.B. and D.D.K. performed the rh*GAA* biodistribution in mice. P.V. and P.S. contributed to the biochemical analyses. M.S.-S., F.C., and S.C. produced the AAV vectors used in the studies. L.v.W. and A.V. performed the delivery of AAV vectors in mice and managed the harvesting of mouse samples. B.G. performed histological staining of mouse muscle. R.H. performed the bioinformatics analyses of protein immunogenicity. F.B., A.M., and C.L. contributed to the studies in NHP.

Competing interests: F.P., P.C., D.D.K., G.R., and F.M. are inventors of patents describing the treatment of Pompe disease with liver gene therapy (acid- α glucosidase variants and uses thereof, application numbers EP16306148, EP16306149, and EP16306150; Immunomodulating gene therapy, WO2009075815). F.C., G.R., M.A.K., and F.M. are inventors of patents describing AAV-mediated liver gene transfer, some of them licensed to commercial companies (AAV capsid proteins for nucleic acid transfer, US20130059732; treatment of hyperbilirubinemia, CA2942451). N.K.P. and M.A.K. are inventors of patents describing the generation of new human hepatotropic AAV capsids (novel recombinant AAV capsids resistant to preexisting human neutralizing antibodies, WO2017143100). P.L., D.D.K., and F.M. have consulted for companies on the topic of Pompe disease and on the development of AAV gene therapies. All other authors declare that they have no competing interests.

⁴Bio-chemical Genetics Laboratory, Duke University Health System, Durham, NC 27710, USA

⁵Departments of Pediatrics and Genetics, Stanford University, Stanford, CA 94305, USA

⁶Paris-Est Neuromuscular Center, Pitié-Salpêtrière Hospital and Raymond Poincaré Teaching Hospital, Garches, APHP, Paris, France

⁷Division of Medical Genetics, Department of Pediatrics and Department of Molecular Genetics and Microbiology, Duke University School of Medicine, Durham, NC 27710, USA

Abstract

Glycogen storage disease type II or Pompe disease is a severe neuromuscular disorder caused by mutations in the lysosomal enzyme, acid α -glucosidase (GAA), which result in pathological accumulation of glycogen throughout the body. Enzyme replacement therapy is available for Pompe disease; however, it has limited efficacy, has high immunogenicity, and fails to correct pathological glycogen accumulation in nervous tissue and skeletal muscle. Using bioinformatics analysis and protein engineering, we developed transgenes encoding GAA that could be expressed and secreted by hepatocytes. Then, we used adeno-associated virus (AAV) vectors optimized for hepatic expression to deliver the *GAA* transgenes to *Gaa* knockout (*Gaa*^{-/-}) mice, a model of Pompe disease. Therapeutic gene transfer to the liver rescued glycogen accumulation in muscle and the central nervous system, and ameliorated cardiac hypertrophy as well as muscle and respiratory dysfunction in the *Gaa*^{-/-} mice; mouse survival was also increased. Secretable GAA showed improved therapeutic efficacy and lower immunogenicity compared to nonengineered GAA. Scale-up to nonhuman primates, and modeling of *GAA* expression in primary human hepatocytes using hepatotropic AAV vectors, demonstrated the therapeutic potential of AAV vector-mediated liver expression of secretable GAA for treating pathological glycogen accumulation in multiple tissues in Pompe disease.

INTRODUCTION

Glycogen storage disease type II, also called Pompe disease (Online Mendelian Inheritance in Man #232300), is an autosomal recessive disorder caused by mutations in the gene encoding the lysosomal enzyme acid α -glucosidase (GAA), which catalyzes the degradation of glycogen. The resulting enzyme deficiency leads to pathological accumulation of glycogen and lysosomal alterations in all tissues of the body, resulting in cardiac, respiratory, and skeletal muscle dysfunction (1). Enzyme replacement therapy with recombinant human GAA (rhGAA) improves survival of patients with the severe infantile form of Pompe disease (2) and stabilizes disease in patients with a late-onset form of the disorder (3, 4). When the enzyme is infused into the circulation, it is taken up by tissues through binding to the cation-independent mannose-6-phosphate receptor on the cell surface (1). However, although a lifesaving therapy for some patients, enzyme replacement therapy has several limitations, leading to treatment failures and limited long-term efficacy. Specifically, the low uptake of the enzyme in skeletal muscle (5) and the inability of rhGAA to cross the blood-brain barrier (BBB) (6), together with the progressive impairment of autophagy (7), limit the ability of enzyme replacement therapy to fully ameliorate the symptoms of Pompe disease. In addition, rhGAA can also induce immune responses, potentially resulting in acute infusion

reactions (4) and development of anti-GAA antibodies (8, 9). This is common in patients with the infantile form of the disease, who frequently develop high-titer antibodies to rhGAA, leading to a poor prognosis (8, 9). In addition, because of the short half-life of rhGAA in tissues, patients are required to undergo frequent, inconvenient, and costly infusions (10).

Gene therapy may be a promising alternative approach to treat Pompe disease. Among gene delivery vectors, clinical experience with adeno-associated virus (AAV) vectors for diseases like hemophilia (11) and congenital blindness (12) has established this system as safe and effective for in vivo gene transfer (13). AAV-based gene therapy has been proposed for expressing the therapeutic *GAA* gene in Pompe disease muscle, the most affected tissue, taking advantage of serotypes endowed with muscle tropism such as AAV9 (14–16), AAV6 (17), and AAV1 (18, 19). A clinical trial of *GAA* gene transfer using AAV1 injected into the diaphragm of patients with Pompe disease has recently been completed (20, 21). The study demonstrated the safety of the approach, although the local delivery limited efficacy to the treated diaphragm muscle (20, 21). Another clinical trial is planned (ClinicalTrials.gov ID: NCT02240407) in which an AAV9 vector, carrying the *GAA* transgene, will be injected intramuscularly in the tibialis anterior of Pompe patients under immunosuppressive regimen (22). Preclinical studies suggest that localized expression of the *GAA* transgene in muscle is associated with incomplete correction of Pompe disease and an enhanced immune response to the GAA protein (15, 23). Therapeutic gene transfer using liver-directed AAV vectors is a potential strategy to achieve correction of Pompe disease across the entire body, based on the ability of hepatocytes to efficiently secrete proteins into the bloodstream. Liver has been successfully targeted using AAV vectors in a variety of preclinical and clinical studies such as those aimed at treating hemophilia B (13). Furthermore, hepatic expression of transgenes, including *GAA*, has been shown to induce antigen-specific immunological tolerance (16, 24, 25).

Liver expression of GAA in a mouse model of Pompe disease resulted in increased enzymatic activity in peripheral tissues (25–27). However, complete correction of glycogen accumulation in tissues difficult to target, such as various skeletal muscles, has not been achieved (28, 29). The use of a chimeric *GAA* transgene containing a heterologous signal peptide from α -1 antitrypsin has been reported to provide better correction of glycogen accumulation in a mouse model of Pompe disease (29). Although these results are promising, high vector doses required to achieve therapeutic efficacy potentially pose a challenge for clinical translation, because they might induce capsid-dependent immunotoxicity (30).

Here, using bioinformatics prediction and protein engineering, we generated a series of *GAA* transgenes and delivered them to mice with Pompe disease using AAV8 vectors, a highly efficient serotype for liver gene transfer (11, 31). Expression of these transgenes resulted in secretion of GAA, high and sustained GAA activity in plasma, enzyme uptake by peripheral tissues, and low immunogenicity in mice. Delivery to non-human primates (NHPs) confirmed both safe and efficient secretion of GAA by the liver and uptake of secreted GAA by peripheral tissues.

RESULTS

Genetic modification of human *GAA* increases enzyme secretion and uptake compared to wild-type *GAA* in Pompe disease model

GAA is a lysosomal enzyme not efficiently secreted by cells (32). To enhance therapeutic efficacy of *GAA* gene transfer, we first developed a codon-optimized version of the human *GAA* complementary DNA (83% nucleotide identity compared to wild-type coding sequence) (fig. S1A). Then, in silico analysis of the *GAA* sequence using the SignalP 4.0 Server (33) predicted that a deletion of at least eight amino acids in the N terminus of the propeptide region of the enzyme would enhance its secretion score (D-score; fig. S1B). On the basis of the in silico prediction, an initial set of wild-type or codon-optimized, deleted (8) *GAA* constructs was cloned (fig. S1A). In addition, the natural secretion signal peptide of the *GAA* protein was replaced by that of the human α -1 antitrypsin enzyme, a highly secreted protein (sp2; fig. S1, A and C) (29). The *GAA* transgenes were cloned in a hepatocyte-specific expression cassette (34) and transiently transfected into the human hepatoma cell line HuH7 (fig. S1, A and C). The codon-optimized, deleted *GAA* construct sp2- 8-co displayed a significant increase in secretion by HuH7 cells compared to both wild-type (** $P < 0.01$) and codon-optimized (* $P < 0.05$) *GAA* transgenes (Fig. 1A).

Then, on the basis of the codon-optimized *GAA* sequence, we generated five additional deleted *GAA* versions carrying signal peptides that were either synthetic (35) or from proteins physiologically secreted from the liver (sp3-8; fig. S1C) and tested them in vitro by transient transfection of HuH7 cells (Fig. 1B). This screening allowed us to identify two additional engineered *GAA* constructs, sp7- 8-co and sp8- 8-co, which provided significantly higher *GAA* activity in cell culture media when compared to both codon-optimized and wild-type *GAA* control transgenes (** $P < 0.001$; Fig. 1B). Western blot analysis of conditioned media showed a 110-kDa band corresponding to the secreted *GAA* precursor (fig. S2A). Higher amounts of secreted *GAA* protein were achieved using sp2- 8-co, sp7- 8-co, and sp8- 8-co constructs compared to the wild-type and codon-optimized *GAA* control constructs (fig. S2A), reflecting *GAA* activity data (Fig. 1B). As predicted by in silico analysis, a deletion up to 42 amino acids (fig. S1B) resulted in *GAA* secretion similar to that of the 8- amino acid deleted *GAA* with no loss of enzyme activity (fig. S2B). Higher secretion of both deleted *GAA* versions was observed when compared to the nonengineered proteins [*** $P < 0.001$ (sp7- 8-co), ** $P < 0.01$ (sp7- 42-co), compared to wt and co] (fig. S2B).

To assess the therapeutic efficacy of the codon-optimized, deleted *GAA* transgenes with the sp7 signal peptide (sp7- 8-co and sp7- 42-co), we performed in vivo gene transfer in *Gaa* knockout (*Gaa*^{-/-}) mice, a model of Pompe disease. The codon-optimized, nondeleted *GAA* trans-gene with the sp7 signal peptide (sp7-co) was used as control. We treated *Gaa*^{-/-} mice by intravenous injection of 2×10^{12} vector genomes (vg)/kg of an AAV8 vector encoding for the different *GAA* versions (Fig. 1, C to E, and fig. S2, C to G). Western blot analysis of mouse plasma 3 months after treatment showed that all the *GAA* protein versions were correctly secreted into the circulation (Fig. 1C), and as expected, the size of the secreted *GAA* precursor was smaller for the deleted sp7- 42-co compared to sp7-co (fig. S2C).

Three months after treatment, corresponding to the plateau of GAA expression, only the sp7- 8-co provided significantly higher circulating amounts of GAA compared to the control [$*P < 0.05$, sp7-co, two-way analysis of variance (ANOVA) time per treatment] (Fig. 1D). This resulted in significantly higher GAA activity in the heart ($*P < 0.05$ compared to sp7-co; Fig. 1E) and quadriceps ($*P < 0.05$ compared to sp7-co; fig. S2D), but not in diaphragm and triceps (fig. S2D). Plasma GAA activity (Fig. 1D) normalized for the amount of GAA protein detected by Western blot (Fig. 1C) was similar for all transgenes (fig. S2E). In the liver of treated animals, GAA activity (fig. S2F) and vector genome copies (fig. S2G) were not significantly different. These results indicate that the deleted secretable *GAA* transgene provided higher circulating GAA and GAA uptake in the heart and quadriceps in *Gaa*^{-/-} mice compared to the nondeleted *GAA* transgene.

AAV-mediated gene transfer of an engineered GAA transgene to mouse liver provides clearance of accumulated glycogen in muscle

On the basis of the results from the initial screening, we assessed the efficacy of gene transfer in vivo in *Gaa*^{-/-} mice with the two best candidates (codon-optimized, deleted *GAA* with heterologous signal peptides: sp2- 8-co and sp7- 8-co). The codon-optimized, nondeleted *GAA* trans-gene with the natural signal peptide, encoding for the native GAA protein (abbreviated as co in the figures), was used as control in all experiments.

To this aim, we generated AAV8 vectors encoding the selected *GAA* constructs under the control of a hepatocyte-specific promoter (hAAT) (34), AAV8-hAAT-co*GAA*, AAV8-hAAT-sp2- 8-co*GAA*, and AAV8-hAAT-sp7- 8-co*GAA* (Fig. 2 and fig. S1C). In all in vivo studies, male *Gaa*^{-/-} mice or wild-type littermates (*Gaa*^{+/+}) were used.

Three independent studies were conducted in which mice were treated at 4 months of age and followed thereafter for 3 or 10 months: (i) a 3-month study treating mice with a low vector dose (5×10^{11} vg/kg), (ii) a 3-month study treating mice with a high vector dose (2×10^{12} vg/kg), and (iii) a 10-month study treating mice with a high vector dose (2×10^{12} vg/kg). Circulating GAA activity was measured 1, 3, and 10 months after treatment (fig. S3A). Plateau activity was reached within 3 months of vector delivery and remained stable for the duration of the observation period (fig. S3A). Circulating GAA activity in plasma was higher in *Gaa*^{-/-} mice treated with AAV vectors expressing the secretable sp- 8-coGAA than in mice treated with the AAV expressing the native GAA at a vector dose of 2×10^{12} vg/kg (Fig. 2A, fig. S3A, and tables S2 and S3). At 5×10^{11} vg/kg, because of the low intrinsic sensitivity of the assay, circulating GAA activity in AAV-treated mice was not changed when compared to mice treated with vehicle (Fig. 2A and table S1). Western blot analysis of mouse plasma showed dose- and transgene-dependent secretion of GAA in plasma, which was significantly higher in animals treated with the secretable version of GAA compared to the native GAA (co: 5×10^{11} vg/kg compared to 2×10^{12} vg/kg, $P = 0.001$; sp7- 8-co: 5×10^{11} vg/kg compared to 2×10^{12} vg/kg, $P = 0.004$; co 2×10^{12} vg/kg compared to sp7- 8-co 2×10^{12} vg/kg, $P = 0.005$; fig. S3, B and C). The differences in enzyme activity between vectors expressing engineered sp- 8-coGAA and native GAA were significant in plasma ($***P < 0.001$, co compared to sp2- 8-co, and $****P < 0.0001$, co compared to sp7- 8-co, 10 months after treatment; Fig. 2A and fig. S3A) but not in liver

(fig. S3D), where the *GAA* transgenes were equally expressed by all vectors. Similar efficiency of liver transduction was found across treatment groups by measuring vector genome copy numbers in the liver (fig. S3E). At sacrifice, 3 and 10 months after gene transfer, *GAA* activity was increased in heart, diaphragm, quadriceps, and triceps of *Gaa*^{-/-} mice treated with the AAV8-*GAA* vectors, compared to vehicle-treated *Gaa*^{-/-} mice, indicating uptake of *GAA* protein from the circulation (Fig. 2B and tables S1 to S3). *GAA* activity in mice treated with AAV vectors encoding secretable *GAA* transgenes at a dose of 2×10^{12} vg/kg was also significantly higher than the endogenous activity measured in *Gaa*^{+/+} control littermates in several tissues, such as heart ($*P < 0.05$ at 3 and 10 months), diaphragm ($*P < 0.05$ at 10 months), quadriceps ($*P < 0.05$ at 3 months), and triceps ($**P < 0.01$ at 3 months) (Fig. 2B and tables S2 and S3). These results evidence supraphysiological uptake of *GAA* in several tissues, resulting from high secretion of engineered *GAA* from the liver. As previously reported (27, 29, 36), the *GAA* activity we achieved after gene therapy was higher in heart and diaphragm compared to quadriceps and triceps, reflecting the variable efficiency of *GAA* uptake from the circulation in these muscle groups (Fig. 2B).

GAA activity in tissues reflected a reduction in glycogen accumulation (Fig. 2C). Three months after gene transfer, a vector dose-dependent correction of glycogen accumulation was observed in diaphragm, quadriceps, and triceps muscle, with a lower glycogen accumulation observed at a vector dose of 2×10^{12} vg/kg compared to a vector dose of 5×10^{11} vg/kg ($P < 0.0001$, two-way ANOVA dose per treatment, dose). At a vector dose of 2×10^{12} vg/kg, treatment with vectors encoding all *GAA* transgenes resulted in robust glycogen reduction in cardiac and skeletal muscles (Fig. 2C). At a vector dose of 5×10^{11} vg/kg, significant differences in glycogen clearance between native and secretable *GAA* were found in the heart ($**P < 0.01$, co compared to sp- 8-co; Fig. 2C). In addition, partial but significant glycogen reduction was observed in triceps isolated from *Gaa*^{-/-} mice treated with the AAV expressing the sp7- 8-co *GAA* transgene ($*P < 0.05$, vehicle-treated compared to sp7- 8-co *Gaa*^{-/-}; Fig. 2C). These findings support the hypothesis that the secretable *GAA* proteins have higher therapeutic efficacy than the native non-engineered *GAA*.

Treatment of *Gaa*^{-/-} animals at a vector dose of 2×10^{12} vg/kg highlighted a time-dependent correction of the Pompe disease phenotype, with more efficient clearance of glycogen in triceps 10 months compared to 3 months after gene delivery ($***P < 0.001$, two-way ANOVA time per treatment; Fig. 2C and tables S2 and S3). Ten months after gene transfer to the liver, reduction in glycogen accumulation was observed in all muscle tissues, including quadriceps and triceps ($****P < 0.0001$, vehicle compared to AAV-treated *Gaa*^{-/-} mice; Fig. 2C and table S3).

AAV-mediated gene transfer of secretable *GAA* to mouse liver preserves muscle structure and normalizes autophagy

Because we observed clearance of glycogen from muscle of *Gaa*^{-/-} mice 10 months after gene delivery, we asked whether this was accompanied by normalization of histological phenotype. Hematoxylin and eosin staining of muscle confirmed no evident morphological abnormalities in muscle fibers of AAV-treated *Gaa*^{-/-} mice, which resembled those of *Gaa*^{+/+} control mice (Fig. 3A and fig. S4). This was accompanied by loss of periodic acid-Schiff

staining for glycogen (Fig. 3A and fig. S4), which reflected the quantitative reduction in glycogen content measured by biochemical assays (Fig. 2C). In $Gaa^{-/-}$ mice, the pathological glycogen accumulation in lysosomes results in the dysfunction of the endolysosomal compartment (7), buildup of autophagy substrates (37), and impaired trafficking of the precursor GAA to lysosomes, where it is processed to a lower molecular weight mature form. By Western blot analysis, we detected both the precursor GAA (110 kDa) and the mature lysosomal GAA (70 to 75 kDa) forms in muscle of animals treated with AAV liver gene transfer (Fig. 3B and fig. S5, A and B), suggesting a normal lysosomal trafficking upon internalization of GAA from the circulation. Notably, the amount of lysosomal GAA protein was significantly higher in triceps muscle of $Gaa^{-/-}$ mice treated with the sp7-8-co vector than with the control vector encoding for native GAA ($***P < 0.001$, lysosomal GAA; Fig. 3, B and C). Next, we evaluated autophagy impairment by measuring the amount of the p62 protein, a recognized marker of autophagy substrate buildup in Pompe disease (37, 38). Western blot analysis was used to measure the accumulation of p62 in triceps and quadriceps muscle of AAV-treated $Gaa^{-/-}$ mice together with vehicle-treated $Gaa^{-/-}$ mice and $Gaa^{+/+}$ control littermates (Fig. 3, D and E, and fig. S5, C and D). The pathological accumulation of p62 was normalized in AAV-treated $Gaa^{-/-}$ mice in both triceps muscle (Fig. 3, D and E) and quadriceps muscle (fig. S5, C and D).

AAV-mediated transfer of secretable GAA to mouse liver improves pathology in mouse brain and spinal cord

We next investigated whether engineered secretable GAA proteins expressed by liver gene transfer could be taken up by cells in the central nervous system, leading to the correction of the disease phenotype (39, 40). Codon-optimized, nondeleted GAA transgene encoding for the native GAA with the native signal peptide was used as control. Ten months after AAV treatment at a high vector dose (2×10^{12} vg/kg), Western blot analyses of whole mouse brain (Fig. 4A and fig. S6A) and spinal cord (Fig. 4B) lysates showed the presence of the 70- to 75-kDa mature lysosomal GAA. At a low vector dose of 5×10^{11} vg/kg, lysosomal GAA was detected in the brains of all mice treated with the secretable GAA, but only in two of five brains of mice treated with the native GAA (fig. S6, B and C). Similar GAA activity was measured in brain across treatment groups at high and low vector doses, possibly reflecting the low intrinsic sensitivity of the assay (tables S1 to S3). At a high vector dose (2×10^{12} vg/kg), a significant reduction of glycogen was measured in the brains of $Gaa^{-/-}$ mice treated with secretable GAA compared to $Gaa^{-/-}$ mice treated with vehicle ($***P < 0.001$, $Gaa^{-/-}$ -vehicle compared to sp2-8-co; $****P < 0.0001$ $Gaa^{-/-}$ -vehicle compared to sp7-8-co; Fig. 4C). As for muscle (Fig. 2C), glycogen clearance in brain improved from 3 to 10 months after gene delivery ($****P < 0.0001$, two-way ANOVA time per treatment; Fig. 4C). There was no significant correction of glycogen in the brains of mice at 3 and 10 months after treatment with the vector encoding for the native GAA protein compared to vehicle-treated mice ($P = 0.20$, $Gaa^{-/-}$ -vehicle compared to co, 10 months after gene delivery; Fig. 4C), although GAA protein was detected in brain (Fig. 4A and tables S2 and S3).

Immunofluorescence analysis of the cervical, thoracic, and lumbar regions of the mouse spinal cord showed increased motor neuron survival in AAV-treated $Gaa^{-/-}$ mice compared

to vehicle-treated $Gaa^{-/-}$ mice ($*P < 0.05$), revealed by staining with choline acetyltransferase (Fig. 4, D and E) and reduced numbers of cells positive for Iba1 (ionized calcium binding adaptor molecule 1), a marker of macrophages and microglia, in AAV-treated $Gaa^{-/-}$ mice compared to vehicle-treated $Gaa^{-/-}$ mice ($***P < 0.001$) (Fig. 4, F and G). Astrogliosis, measured by quantification of GFAP (glial fibrillary acidic protein) staining in the spinal cord gray matter, was normalized by treatment with the secretable GAA transgene product when compared to $Gaa^{+/+}$ control mice (Fig. 4, H and I).

Secretable GAA is less immunogenic than native GAA

rhGAA is known to induce neutralizing humoral immune responses in patients with Pompe disease undergoing enzyme replacement therapy (8, 9). We therefore measured anti-human GAA immunoglobulin G (IgG) in the plasma of $Gaa^{-/-}$ mice treated with the AAV vector (either 5×10^{11} or 2×10^{12} vg/kg) expressing secretable GAA. These mice did not develop anti-GAA IgG 1 month after gene delivery, whereas mice treated with the vectors encoding for the native GAA protein did (anti-GAA IgGs were up to 22 and 6 $\mu\text{g/ml}$ for the low and high vector dose groups, respectively; 5×10^{11} vg/kg: native GAA, co, compared to sp2- 8-co, $P = 0.004$; native GAA, co, compared to sp7- 8-co, $P = 0.006$; Fig. 5A). Time-course evaluation of antibody responses to the GAA transgene product in the high vector dose (2×10^{12} vg/kg) group indicated a transient humoral immune response to native GAA that disappeared 3 months after liver gene transfer (Fig. 5B). Higher immunogenicity of native GAA compared to secretable GAA was observed 1 month after injection but not at later time points ($P = 0.035$, native GAA, co, compared to sp2- 8-co; $P = 0.022$, native GAA, co, compared to sp7- 8-co; Fig. 5B). To further investigate the immunogenicity of secretable GAA compared to the native GAA, we expressed the native and secretable GAA transgenes under the control of a muscle-specific promoter (SPc5-12) (41). One month after AAV gene delivery (2×10^{12} vg/kg), mice treated with the vectors encoding for the native GAA protein developed anti-GAA IgG (three of four mice; average IgG, 12 $\mu\text{g/ml}$), whereas mice treated with the vectors encoding for secretable GAA protein developed low anti-GAA IgG (two of five mice; average IgG, 2.4 $\mu\text{g/ml}$; fig. S7); however, these differences were not statistically significant due to variability of the response.

To investigate the potential immunogenicity of the secretable GAA transgene product in humans, bioinformatics analysis was performed to identify potential class II major histocompatibility complex (MHC II) epitopes in the GAA protein. Analysis of the Immune Epitope Database (www.iedb.org) identified the epitope LHDFLVPRELSGSS as the best predicted binder to the human leukocyte antigen (HLA) allele DRB1 and particularly for haplotypes DRB1*03:01, DRB1*04:03, DRB1*07:01, DRB1*11:01, and DRB1*15:01, which are found on 50% of the human population (42). This epitope, located at amino acid 32 of the GAA sequence, is not present in the secretable GAA protein.

Secretable GAA ameliorates the disease phenotype and improves long-term survival in a Pompe disease mouse model

AAV-mediated transfer of the *GAA* transgene to mouse liver improved the survival of $Gaa^{-/-}$ mice, regardless of the *GAA* transgene version expressed (Fig. 6A). AAV-treated $Gaa^{-/-}$ mice displayed normal weight gain over time (fig. S8). Cardiac hypertrophy was present in

all $Gaa^{-/-}$ animals at the time of vector infusion (fig. S9A) but was rescued in animals receiving vectors encoding for native or secretable GAA proteins (Fig. 6B). AAV vector-mediated gene delivery to liver also resulted in long-term preservation of muscle strength in $Gaa^{-/-}$ mice as revealed by the wire hang test, whereas vehicle-treated $Gaa^{-/-}$ mice showed a progressive deterioration from baseline to month 10 after treatment (Fig. 6C and figs. S9B and S10A). Gene transfer also rescued impairment in the grip test in $Gaa^{-/-}$ mice (Fig. 6D and figs. S9C and S10B). Improvements in wire hang performance were observed in mice treated with vectors encoding for both native and secretable GAA (Fig. 6C), whereas in the grip test, only animals treated with secretable GAA showed rescue compared to $Gaa^{-/-}$ mice treated with vehicle ($Gaa^{-/-}$ -vehicle compared to sp2- 8-co, $P=0.009$; $Gaa^{-/-}$ -vehicle compared to sp7- 8-co, $P=0.005$; Fig. 6D). No significant differences were seen in the rotarod test in our $Gaa^{-/-}$ model of Pompe disease (figs. S9D and S10C).

Respiratory function in $Gaa^{-/-}$ mice is known to be impaired (39). Because of the low survival of vehicle-treated $Gaa^{-/-}$ mice (3 of 10; Fig. 6A) and the likely selection of animals with a slightly milder phenotype, the 10-month measurement of tidal volume by plethysmography of long-lived vehicle-treated $Gaa^{-/-}$ mice did not differ significantly from $Gaa^{+/+}$ control mice ($P=0.38$; Fig. 6E). Despite this, treatment of $Gaa^{-/-}$ mice with the vectors encoding for secretable sp7- 8-coGAA led to higher ventilation compared to those treated with vectors encoding for native GAA ($*P<0.05$; Fig. 6E and table S4).

Gene delivery of AAV8-sp7- 8-coGAA leads to increased GAA activity in plasma and tissues of NHPs

We treated three healthy NHP (*Macaca fascicularis*) with AAV8 vectors encoding the sp7- 8-coGAA transgene at a vector dose of 2×10^{12} vg/kg (Fig. 7). Secretion of the engineered GAA protein from the liver into the circulation was confirmed by Western blot analysis (Fig. 7A), which showed the GAA trans-gene product in plasma collected at 30 and 90 days after AAV injection. In the treated animals, circulating GAA activity was increased by about three- to sixfold above the baseline measured in a control NHP cohort ($**P<0.01$) and remained stable until the end of the study (90 days after treatment; Fig. 7B). Circulating GAA (Fig. 7, A and B) was consistent with the efficiency of liver transduction as assessed by vector genome copy number (fig. S11). Given that wild-type NHPs physiologically express GAA in all tissues, we used six control animals injected with an unrelated AAV vector as a reference for endogenous GAA activity in the tissues (Fig. 7C). At 3 months after treatment, in animals injected with AAV8-sp7- 8-coGAA (AAV-GAA), enzyme activity was increased compared to control animals in heart ($***P<0.001$), diaphragm ($*P<0.05$), and triceps ($*P<0.05$) (Fig. 7C). These results demonstrate that the engineered sp7- 8-coGAA transgene was expressed in the liver of an NHP large-animal model and that the protein product was secreted into the circulation and taken up by peripheral tissues.

Delivery of sp7- 8-coGAA to liver induces long-lasting GAA activity in a mouse model of Pompe disease

Pompe disease is currently managed by infusions of rhGAA protein at 20 to 40 mg/kg every other week (5). Upon infusion, the recombinant enzyme is rapidly cleared from the circulation and is mostly taken up by the liver and heart and less efficiently by other tissues

(1). To evaluate whether stable plasma GAA activity provided by AAV vector-mediated gene transfer to liver resulted in accumulation of GAA in muscle of *Gaa*^{-/-} mice, we correlated GAA activity in plasma with that measured in heart, diaphragm, quadriceps, and triceps muscles (Fig. 8A and tables S1 and S2). Linear regression revealed a correlation ($r^2 > 0.7$ in all muscle groups) between plasma and tissue GAA activity and confirmed that GAA was preferentially taken up by heart, followed by diaphragm and skeletal muscle, as indicated by the slope of the regression curves (Fig. 8A).

Next, we compared GAA activity obtained after rhGAA enzyme replacement therapy in *Gaa*^{-/-} mice with that measured after AAV gene therapy in *Gaa*^{-/-} mice and NHPs. *Gaa*^{-/-} mice received a high vector dose of rhGAA (100 mg/kg, two infusions total, given every other week) corresponding to 2.5- to 5-fold the rhGAA used in enzyme replacement therapy in human patients (5). We then sacrificed the rhGAA-treated mice at defined time points after the last infusion, and tissues were collected for GAA activity measurements in heart (Fig. 8B) and triceps muscle (Fig. 8C). As expected, rhGAA uptake was more efficient in heart compared to triceps muscle in *Gaa*^{-/-} mice (Fig. 8, B and C). GAA activity in tissues returned to baseline within ~30 to 40 days after the last rhGAA infusion (Fig. 8, B and C), with an estimated half-life of GAA in heart and triceps muscle of 5.85 and 2.03 days, respectively. We then compared the GAA activity achieved in heart and triceps with our candidate sp7-8-coGAA transgene by liver gene therapy in *Gaa*^{-/-} mice and NHPs (Figs. 2B and 7) to that measured in the same tissues of *Gaa*^{-/-} mice after rhGAA treatment (Fig. 8, B and C). The GAA activity in heart and triceps muscle measured 3 months after vector injection in *Gaa*^{-/-} mice at the high vector dose (2×10^{12} vg/kg) was similar to the GAA activity 1 to 3 days after the infusion of rhGAA. At the low vector dose (5×10^{11} vg/kg), GAA activity in heart and triceps muscle measured 3 months after vector injection in *Gaa*^{-/-} mice was similar to that measured in NHPs and equivalent to that measured in *Gaa*^{-/-} mice ~15 days after the infusion of high-dose rhGAA (Fig. 8, B and C).

As improving liver transduction by the AAV vector would increase transgene expression and allow the use of lower vector doses, we packaged the hAAT-sp7-8-coGAA transgene expression cassette in several different AAV serotypes and screened them in vitro using primary hepatocytes derived from NHPs (Fig. 8D) and human donors (Fig. 8E). We compared the AAV serotypes with AAV8, the best-characterized serotype for liver transduction in humans (11, 43). Three serotypes—AAV3B (44), AAVLK03 (45), and the newly developed serotype AAVNP59 (46)—showed improved transduction efficiency (Fig. 8, D and E), with AAVLK03 showing significantly higher transgene expression compared to AAV8 in human primary hepatocytes (* $P < 0.05$, AAVLK03 compared to AAV8; Fig. 8E).

DISCUSSION

The high amounts of rhGAA enzyme required to correct the Pompe disease phenotype (47) and the immunogenicity of GAA (8) are important limitations of enzyme replacement therapy. A challenge for GAA gene therapy is that most of the protein traffics to lysosomes and is not secreted (32), potentially accounting for only partial efficacy in mouse models after in vivo (18, 26, 27, 48) and ex vivo gene therapy (49). Here, we report therapeutic GAA transgene expression in the liver of a mouse model of Pompe disease, which resulted

in the correction of glycogen accumulation in multiple tissues at AAV vector doses already tested in the clinic in the context of liver gene transfer trials (11).

Gene delivery to muscle has been proposed as a treatment for Pompe disease (14–19). In the only gene therapy clinical trial performed so far, the diaphragm was directly targeted by intraparenchymal injection of an AAV1 vector encoding a *GAA* transgene (20, 21). The localized treatment was well tolerated but only resulted in improvements in the targeted region (20, 21), reflecting that achieving significant levels of transgene secretion in plasma by intramuscular vector delivery is challenging, as indicated by an early gene therapy clinical trial for hemophilia (50). Systemic delivery of AAV vectors has been tested in murine models of Pompe disease (15). However, large-animal studies for other enzyme deficiency diseases indicate that greatly elevated vector doses ($>10^{14}$ vg/kg) are needed to correct neuromuscular deficits throughout the body (51, 52). This poses important constraints in terms of both potential immunotoxicities (30) and vector manufacturing.

Here, low vector doses (5×10^{11} vg/kg) of AAV8 vectors encoding for secretable GAA proteins resulted in clearance of glycogen in *Gaa*^{-/-} mouse heart, with ~50% reduction in glycogen in diaphragm, quadriceps, and triceps muscle. A fivefold increase in vector dose (2×10^{12} vg/kg) resulted in glycogen clearance from all muscles 3 months after treatment with vectors encoding for both native and secretable GAA, demonstrating a clear dose response. Furthermore, longer follow-up of animals highlighted a time-dependent effect of GAA expression on therapeutic efficacy, with better clearance of glycogen in several tissues 10 months compared to 3 months after treatment. This indicates that not only the dose but also the time of continuous exposure to GAA are important for reversal of the Pompe phenotype.

Clearance of accumulated glycogen in different muscle types resulted in improved function and an increased survival of Pompe mice. Notably, mice were administered gene therapy at 4 months of age, when glycogen had already accumulated in all tissues (48, 53) and the animals were showing signs of cardiac hypertrophy and mild muscle weakness. In our experimental cohort, respiratory function in untreated *Gaa*^{-/-} mice was not significantly impaired compared to *Gaa*^{+/+} healthy litter-mates, reflecting the fact that most *Gaa*^{-/-} mice died and those left had a mild phenotype. Treatment with vector expressing the secretable sp7-8-co*GAA* transgene resulted in a better respiratory performance when compared to animals treated with vectors expressing native GAA.

Analysis of muscle glycogen content in treated mice showed that there was a threshold of circulating GAA activity required for glycogen clearance. This threshold was lower for the heart than for diaphragm, quadriceps, and triceps muscles. In the spinal cord, whereas survival of motor neurons and neuroinflammation were improved by vectors encoding for both native and secretable GAA, normalization of astrogliosis required higher circulating GAA activity, which was obtained only with secretable GAA. A similar trend was observed in the accumulation of the autophagic marker p62, which was lower in animals with higher muscle GAA activity after treatment. These results are in agreement with data showing that the combination of enzyme replacement therapy with chaperones, leading to a longer half-life of the stabilized rhGAA protein, results in greater therapeutic efficacy (54).

We found the GAA protein in both brain and spinal cord of the treated *Gaa*^{-/-} mice. As with infused rhGAA, the GAA secreted by liver does not normally cross the BBB (6). However, as reported for other lysosomal enzymes, high circulating GAA may lead to leakage across the BBB (55). Other mechanisms such as transport via exosomes (56) or lysosomal exocytosis at neuromuscular junctions potentially may also be involved (57).

Another key feature of targeting the *GAA* transgene to liver is that *GAA* expression in hepatocytes results in induction of immunological tolerance (24). This has been shown in Pompe disease mouse model (16, 25, 58, 59) and has been used to eradicate established immune responses to clotting factors in hemophilia B mouse and dog models (60, 61). Our data show that secretable GAA proteins have a decreased immunogenicity profile compared to the native GAA protein when expressed not only in liver but also in muscle.

One possible limitation of our approach is related to the persistence of *GAA* expression after liver gene transfer in young pediatric patients with Pompe disease. Although no clinical data are available to date, results in neonatal mice suggest that, after AAV vector-mediated gene transfer, therapeutic efficacy is at least partially lost as the liver grows (34, 62). Future clinical translation efforts will have to address transgene persistence in the liver of pediatric patients (34) and potentially the need for vector read-ministration (22, 63). Nevertheless, the scale-up of our approach to NHPs supports the safety and feasibility of the approach in humans.

In conclusion, AAV liver gene transfer with engineered GAA resulted in therapeutic efficacy at low vector doses, reduced anti-GAA immune responses, and efficient secretion and uptake in a large-animal model. This bodes well for the future translation of this gene therapy approach for the treatment of Pompe disease.

MATERIALS AND METHODS

Study design

To evaluate the therapeutic effect of liver-mediated gene transfer for the treatment of Pompe disease, male *Gaa* knockout (*Gaa*^{-/-}) mice were injected intravenously with AAV vectors encoding for native or engineered GAA proteins at 4 months of age, when the animals showed already significant accumulation of glycogen in all tissues. Male healthy littermates expressing wild-type *Gaa* (*Gaa*^{+/+}) were used as controls. Therapeutic readouts were tissue glycogen content, GAA enzyme activity, histological evaluation, and muscle and respiratory function analyses. Experimental groups were sized to allow for statistical analysis; all the animals were included in the analysis, and none of the outliers was excluded. Mice were assigned randomly to the experimental groups, and the operators who performed vector delivery and functional analyses were blinded to group identity.

In vivo studies

Mouse studies were performed according to the French and European legislation on animal care and experimentation (2010/63/EU) and approved by the local institutional ethical committee (protocol no. 2015-008). The mouse procedures involving the administration of rhGAA were performed at Duke University and approved by the local Institutional Animal

Care and Use Committee. $Gaa^{-/-}$ mice were purchased from the Jackson Laboratory (B6;129-Gaam1Rabn/J, stock no. 004154, 6neo) and were originally generated by Raben and colleagues (53). AAV vectors were administered intravenously via the tail vein.

The kinetic of clearance of the GAA enzyme in heart and triceps was evaluated in 2-month-old $Gaa^{-/-}$ mice after two intravenous injections of rhGAA at 100 mg/kg 1 week apart. Groups of four to five mice were sacrificed 1, 3, 7, 14, 28, and 42 days after the second injection, and heart and triceps were analyzed for residual GAA activity.

For the NHP study, three AAV8 seronegative (64) male animals (*M. fascicularis*) were included in the study. Animals were housed and in vivo procedures were conducted at the Nantes-Atlantic National College of Veterinary Medicine, Food Science and Engineering (Oniris, Nantes, France). Animals were handled according to French and European legislation on animal care 2010/63/EU. The protocol was approved by the local institutional ethical committee (APAFIS#2651-2015110216583210v5). AAV vectors were administered by systemic injection into the saphenous vein of anesthetized animals. Vector was infused in a volume of 24 ml over the course of 1 hour. Two of the three animals received one intravenous infusion of rapamycin (2 mg/kg) the day of vector infusion.

As a baseline readout of GAA enzyme activity in tissues of wild-type NHPs, tissues from six control monkeys treated with an unrelated AAV vector were used. For plasma, baseline GAA activity from eight NHPs was averaged.

Statistical analysis

All the data shown in the present study are reported as means \pm SD. The number of sampled units, n , upon which we reported statistic, is the single mouse for the in vivo experiments (one mouse is $n = 1$) and the single independent experiment for the in vitro studies using cell lines (one independent experiment is $n = 1$). GraphPad Prism 6 software (GraphPad Software) was used for statistical analyses. $P < 0.05$ was considered significant. For all the data sets, data were analyzed by parametric tests, $\alpha = 0.05$ (one- and two-way ANOVA with Tukey's or Dunnett's post hoc correction and multiple t tests with Sidak-Bonferroni post hoc correction). Nonparametric tests were performed when only two groups were compared (unpaired t test). The survival of $Gaa^{-/-}$ mice was compared by Kaplan-Meier log-rank test. The statistical analysis performed for each data set is indicated in the figure legends. For all figures, * $P < 0.05$, ** $P < 0.01$, *** $P < 0.001$, **** $P < 0.0001$, except where different symbols were used.

Supplementary Material

Refer to Web version on PubMed Central for supplementary material.

Acknowledgments

We thank the Oniris platform and E. Ayuso for helping us with the NHP studies.

Funding: This work was supported by a Genethon and the French Muscular Dystrophy Association (AFM). It was also supported by the European Union's research and innovation program under grant agreement nos. 667751 (to F.M.) and 658712 (to F.M. and G.R.), the European Research Council Consolidator Grant under grant agreement

no. 617432 (to F.M.), ASTRE (Action de soutien a la technologie et a la recherche en Esssonne) grant (to F.M.), a grant from Genethon (to D.D.K.), and NIH grant R01-HL092096 (to M.A.K.). N.K.P. was supported by postdoctoral fellowships from NIH (F32-HL119059), the American Liver Foundation Hans Popper Memorial Fellowship, and the Stanford Dean's Fellowship. This project was also supported, in part, by NIH Shared Instrumentation Grant (S10-OD01058001-A1) from the National Center for Research Resources (NCRR) with significant contribution from Stanford's Beckman Center. The plethysmography equipment was acquired with funds from the "Fonds pour le Rayonnement de la Recherche," Université d'Evry. The contents of this publication are solely the responsibility of the authors and do not necessarily represent the official views of the NCRR, NIH, Stanford University, Genethon, or the AFM.

REFERENCES AND NOTES

- van der Ploeg AT, Reuser AJJ. Pompe's disease. *Lancet*. 2008; 372:1342–1353. [PubMed: 18929906]
- Kishnani PS, Corzo D, Nicolino M, Byrne B, Mandel H, Hwu WL, Leslie N, Levine J, Spencer C, McDonald M, Li J, Dumontier J, Halberthal M, Chien YH, Hopkin R, Vijayaraghavan S, Gruskin D, Bartholomew D, van der Ploeg A, Clancy JP, Parini R, Morin G, Beck M, De la Gastine GS, Jokic M, Thurberg B, Richards S, Bali D, Davison M, Worden MA, Chen YT, Wraith JE. Recombinant human acid α -glucosidase: Major clinical benefits in infantile-onset Pompe disease. *Neurology*. 2007; 68:99–109. [PubMed: 17151339]
- Schoser B, Stewart A, Kanters S, Hamed A, Jansen J, Chan K, Karamouzian M, Toscano A. Survival and long-term outcomes in late-onset Pompe disease following α -glucosidase alfa treatment: A systematic review and meta-analysis. *J Neurol*. 2017; 264:621–630. [PubMed: 27372449]
- van der Ploeg AT, Clemens PR, Corzo D, Escolar DM, Florence J, Groeneveld GJ, Herson S, Kishnani PS, Laforet P, Lake SL, Lange DJ, Leshner RT, Mayhew JE, Morgan C, Nozaki K, Park DJ, Pestronk A, Rosenbloom B, Skrinar A, van Capelle CI, van der Beek NA, Wasserstein M, Zivkovic SA. A randomized study of α -glucosidase alfa in late-onset Pompe's disease. *N Engl J Med*. 2010; 362:1396–1406. [PubMed: 20393176]
- Kishnani PS, Beckemeyer AA. New therapeutic approaches for Pompe disease: Enzyme replacement therapy and beyond. *Pediatr Endocrinol Rev*. 2014; 12(suppl 1):114–124. [PubMed: 25345093]
- Ebbink BJ, Poelman E, Plug I, Lequin MH, van Doorn PA, Aarsen FK, van der Ploeg AT, van den Hout JMP. Cognitive decline in classic infantile Pompe disease: An underacknowledged challenge. *Neurology*. 2016; 86:1260–1261. [PubMed: 26944269]
- Fukuda T, Ahearn M, Roberts A, Mattaliano RJ, Zaal K, Ralston E, Plotz PH, Raben N. Autophagy and mistargeting of therapeutic enzyme in skeletal muscle in Pompe disease. *Mol Ther*. 2006; 14:831–839. [PubMed: 17008131]
- Kishnani PS, Goldenberg PC, DeArme SL, Heller J, Benjamin D, Young S, Bali D, Smith SA, Li JS, Mandel H, Koeberl D, Rosenberg A, Chen Y-T. Cross-reactive immunologic material status affects treatment outcomes in Pompe disease infants. *Mol Genet Metab*. 2010; 99:26–33. [PubMed: 19775921]
- de Vries JM, van der Beek NAME, Kroos MA, Özkan L, van Doorn PA, Richards SM, Sung CCC, Brugma J-DC, Zandbergen AAM, van der Ploeg AT, Reuser AJJ. High antibody titer in an adult with Pompe disease affects treatment with α -glucosidase alfa. *Mol Genet Metab*. 2010; 101:338–345. [PubMed: 20826098]
- Kanters TA, Hoogenboom-Plug I, Rutten-Van Mülken MPMH, Redekop WK, van der Ploeg AT, Hakkaart L. Cost-effectiveness of enzyme replacement therapy with α -glucosidase alfa in classic infantile patients with Pompe disease. *Orphanet J Rare Dis*. 2014; 9:75. [PubMed: 24884717]
- Nathwani AC, Tuddenham EGD, Rangarajan S, Rosales C, McIntosh J, Linch DC, Chowdary P, Riddell A, Pie AJ, Harrington C, O'Beirne J, Smith K, Pasi J, Glader B, Rustagi P, Ng CY, Kay MA, Zhou J, Spence Y, Morton CL, Allay J, Coleman J, Sleep S, Cunningham JM, Srivastava D, Basner-Tschakarjan E, Mingozzi F, High KA, Gray JT, Reiss UM, Nienhuis AW, Davidoff AM. Adenovirus-associated virus vector-mediated gene transfer in hemophilia B. *N Engl J Med*. 2011; 365:2357–2365. [PubMed: 22149959]

12. Maguire AM, Simonelli F, Pierce EA, Pugh EN Jr, Mingozzi F, Bennicelli J, Banfi S, Marshall KA, Testa F, Surace EM, Rossi S, Lyubarsky A, Arruda VR, Konkle B, Stone E, Sun J, Jacobs J, Dell'Osso L, Hertle R, Ma J-x, Redmond TM, Zhu X, Hauck B, Zeleniaia O, Shindler KS, Maguire MG, Wright JF, Volpe NJ, McDonnell JW, Auricchio A, High KA, Bennett J. Safety and efficacy of gene transfer for Leber's congenital amaurosis. *N Engl J Med*. 2008; 358:2240–2248. [PubMed: 18441370]
13. Mingozzi F, High KA. Therapeutic in vivo gene transfer for genetic disease using AAV: Progress and challenges. *Nat Rev Genet*. 2011; 12:341–355. [PubMed: 21499295]
14. Sun B, Young SP, Li P, Di C, Brown T, Salva MZ, Li S, Bird A, Yan Z, Auten R, Hauschka SD, Koeberl DD. Correction of multiple striated muscles in murine Pompe disease through adeno-associated virus-mediated gene therapy. *Mol Ther*. 2008; 16:1366–1371. [PubMed: 18560415]
15. Falk DJ, Soustek MS, Todd AG, Mah CS, Cloutier DA, Kelley JS, Clement N, Fuller DD, Byrne BJ. Comparative impact of AAV and enzyme replacement therapy on respiratory and cardiac function in adult Pompe mice. *Mol Ther Methods Clin Dev*. 2015; 2:15007. [PubMed: 26029718]
16. Doerfler PA, Todd AG, Clement N, Falk DJ, Nayak S, Herzog RW, Byrne BJ. Copackaged AAV9 vectors promote simultaneous immune tolerance and phenotypic correction of Pompe disease. *Hum Gene Ther*. 2016; 27:43–59. [PubMed: 26603344]
17. Sun B, Zhang H, Franco LM, Brown T, Bird A, Schneider A, Koeberl DD. Correction of glycogen storage disease type II by an adeno-associated virus vector containing a muscle-specific promoter. *Mol Ther*. 2005; 11:889–898. [PubMed: 15922959]
18. Fraites TJ Jr, Schleissing MR, Shanely RA, Walter GA, Cloutier DA, Zolotukhin I, Pauly DF, Raben N, Plotz PH, Powers SK, Kessler PD, Byrne BJ. Correction of the enzymatic and functional deficits in a model of Pompe disease using adeno-associated virus vectors. *Mol Ther*. 2002; 5:571–578. [PubMed: 11991748]
19. Mah C, Cresawn KO, Fraites TJ Jr, Pacak CA, Lewis MA, Zolotukhin I, Byrne BJ. Sustained correction of glycogen storage disease type II using adeno-associated virus serotype 1 vectors. *Gene Ther*. 2005; 12:1405–1409. [PubMed: 15920463]
20. Smith BK, Martin AD, Lawson LA, Vernot V, Marcus J, Islam S, Shafi N, Corti M, Collins SW, Byrne BJ. Inspiratory muscle conditioning exercise and diaphragm gene therapy in Pompe disease: Clinical evidence of respiratory plasticity. *Exp Neurol*. 2017; 287:216–224. [PubMed: 27453480]
21. Byrne PI, Collins S, Mah CC, Smith B, Conlon T, Martin SD, Corti M, Cleaver B, Islam S, Lawson LA. Phase I/II trial of diaphragm delivery of recombinant adeno-associated virus acid alpha-glucosidase (rAAV1-CMV-*GAA*) gene vector in patients with Pompe disease. *Hum Gene Ther Clin Dev*. 2014; 25:134–163. [PubMed: 25238277]
22. Corti M, Cleaver B, Clément N, Conlon TJ, Farris KJ, Wang G, Benson J, Tarantal AF, Fuller D, Herzog RW, Byrne BJ. Evaluation of readministration of a recombinant adeno-associated virus vector expressing acid alpha-glucosidase in Pompe disease: Preclinical to clinical planning. *Hum Gene Ther Clin Dev*. 2015; 26:185–193. [PubMed: 26390092]
23. Sun B, Zhang H, Franco LM, Young SP, Schneider A, Bird A, Amalfitano A, Chen Y-T, Koeberl DD. Efficacy of an adeno-associated virus 8-pseudotyped vector in glycogen storage disease type II. *Mol Ther*. 2005; 11:57–65. [PubMed: 15585406]
24. Mingozzi F, Liu Y-L, Dobrzynski E, Kaufhold A, Liu JH, Wang Y, Arruda VR, High KA, Herzog RW. Induction of immune tolerance to coagulation factor IX antigen by in vivo hepatic gene transfer. *J Clin Invest*. 2003; 111:1347–1356. [PubMed: 12727926]
25. Franco LM, Sun B, Yang X, Bird A, Zhang H, Schneider A, Brown T, Young SP, Clay TM, Amalfitano A, Chen YT, Koeberl DD. Evasion of immune responses to introduced human acid α -glucosidase by liver-restricted expression in glycogen storage disease type II. *Mol Ther*. 2005; 12:876–884. [PubMed: 16005263]
26. Sun B, Chen Y-T, Bird A, Xu F, Hou Y-X, Amalfitano A, Koeberl DD. Packaging of an AAV vector encoding human acid α -glucosidase for gene therapy in glycogen storage disease type II with a modified hybrid adenovirus-AAV vector. *Mol Ther*. 2003; 7:467–477. [PubMed: 12727109]
27. Ziegler RJ, Bercury SD, Fidler J, Zhao MA, Foley J, Taksir TV, Ryan S, Hodges BL, Scheule RK, Shihabuddin LS, Cheng SH. Ability of adeno-associated virus serotype 8-mediated hepatic expression of acid α -glucosidase to correct the biochemical and motor function deficits of

- presymptomatic and symptomatic Pompe mice. *Hum Gene Ther.* 2008; 19:609–621. [PubMed: 18500944]
28. Raben N, Jatkar T, Lee A, Lu N, Dwivedi S, Nagaraju K, Plotz PH. Glycogen stored in skeletal but not in cardiac muscle in acid α -glucosidase mutant (Pompe) mice is highly resistant to transgene-encoded human enzyme. *Mol Ther.* 2002; 6:601–608. [PubMed: 12409258]
 29. Sun B, Zhang H, Benjamin DK Jr, Brown T, Bird A, Young SP, McVie-Wylie A, Chen Y-T, Koeberl DD. Enhanced efficacy of an AAV vector encoding chimeric, highly secreted acid α -glucosidase in glycogen storage disease type II. *Mol Ther.* 2006; 14:822–830. [PubMed: 16987711]
 30. Mingozzi F, High KA. Immune responses to AAV vectors: Overcoming barriers to successful gene therapy. *Blood.* 2013; 122:23–36. [PubMed: 23596044]
 31. Nathwani AC, Reiss UM, Tuddenham EG, Rosales C, Chowdary P, McIntosh J, Della Peruta M, Lheriteau E, Patel N, Raj D, Riddell A, Pie J, Rangarajan S, Bevan D, Recht M, Shen Y-M, Halka KG, Basner-Tschakarjan E, Mingozzi F, High KA, Allay J, Kay MA, Ng CYC, Zhou J, Cancio M, Morton CL, Gray JT, Srivastava D, Nienhuis AW, Davidoff AM. Long-term safety and efficacy of factor IX gene therapy in hemophilia B. *N Engl J Med.* 2014; 371:1994–2004. [PubMed: 25409372]
 32. Hille-Rehfeld A. Mannose 6-phosphate receptors in sorting and transport of lysosomal enzymes. *Biochim Biophys Acta.* 1995; 1241:177–194. [PubMed: 7640295]
 33. Petersen TN, Brunak S, von Heijne G, Nielsen H. SignalP 4.0: Discriminating signal peptides from transmembrane regions. *Nat Methods.* 2011; 8:785–786. [PubMed: 21959131]
 34. Ronzitti G, Bortolussi G, van Dijk R, Collaud F, Charles S, Leborgne C, Vidal P, Martin S, Gjata B, Sola MS, van Wittenberghe L, Vignaud A, Veron P, Bosma PJ, Muro AF, Mingozzi F. A translationally optimized AAV-UGT1A1 vector drives safe and long-lasting correction of Crigler-Najjar syndrome. *Mol Ther Methods Clin Dev.* 2016; 3:16049. [PubMed: 27722180]
 35. Stern B, Optun A, Liesenfeld M, Gey C, Gräfe M, Pryme IF. Enhanced protein synthesis and secretion using a rational signal-peptide library approach as a tailored tool. *BMC Proc.* 2011; 5(suppl 8):O13. [PubMed: 22373211]
 36. Raben N, Fukuda T, Gilbert AL, de Jong D, Thurberg BL, Mattaliano RJ, Meikle P, Hopwood JJ, Nagashima K, Nagaraju K, Plotz PH. Replacing acid α -glucosidase in Pompe disease: Recombinant and transgenic enzymes are equipotent, but neither completely clears glycogen from type II muscle fibers. *Mol Ther.* 2005; 11:48–56. [PubMed: 15585405]
 37. Raben N, Hill V, Shea L, Takikita S, Baum R, Mizushima N, Ralston E, Plotz P. Suppression of autophagy in skeletal muscle uncovers the accumulation of ubiquitinated proteins and their potential role in muscle damage in Pompe disease. *Hum Mol Genet.* 2008; 17:3897–3908. [PubMed: 18782848]
 38. Nascimbeni AC, Fanin M, Masiero E, Angelini C, Sandri M. The role of autophagy in the pathogenesis of glycogen storage disease type II (GSDII). *Cell Death Differ.* 2012; 19:1698–1708. [PubMed: 22595755]
 39. DeRuisseau LR, Fuller DD, Qiu K, DeRuisseau KC, Donnelly WH Jr, Mah C, Reier PJ, Byrne BJ. Neural deficits contribute to respiratory insufficiency in Pompe disease. *Proc Natl Acad Sci USA.* 2009; 106:9419–9424. [PubMed: 19474295]
 40. Turner SMF, Hoyt AK, ElMallah MK, Falk DJ, Byrne BJ, Fuller DD. Neuropathology in respiratory-related motoneurons in young Pompe (*Gaa*^{-/-}) mice. *Respir Physiol Neurobiol.* 2016; 227:48–55. [PubMed: 26921786]
 41. Li X, Eastman EM, Schwartz RJ, Draghia-Akli R. Synthetic muscle promoters: Activities exceeding naturally occurring regulatory sequences. *Nat Biotechnol.* 1999; 17:241–245. [PubMed: 10096290]
 42. Nielsen M, Lundegaard C, Lund O. Prediction of MHC class II binding affinity using SMM-align, a novel stabilization matrix alignment method. *BMC Bioinformatics.* 2007; 8:238. [PubMed: 17608956]
 43. Nietupski JB, Hurlbut GD, Ziegler RJ, Chu Q, Hodges BL, Ashe KM, Bree M, Cheng SH, Gregory RJ, Marshall J, Scheule RK. Systemic administration of AAV8- α -galactosidase A induces humoral

- tolerance in nonhuman primates despite low hepatic expression. *Mol Ther.* 2011; 19:1999–2011. [PubMed: 21712814]
44. Li S, Ling C, Zhong L, Li M, Su Q, He R, Tang Q, Greiner DL, Shultz LD, Brehm MA, Flotte TR, Mueller C, Srivastava A, Gao G. Efficient and targeted transduction of nonhuman primate liver with systemically delivered optimized AAV3B vectors. *Mol Ther.* 2015; 23:1867–1876. [PubMed: 26403887]
45. Lisowski L, Dane AP, Chu K, Zhang Y, Cunningham SC, Wilson EM, Nygaard S, Grompe M, Alexander IE, Kay MA. Selection and evaluation of clinically relevant AAV variants in a xenograft liver model. *Nature.* 2014; 506:382–386. [PubMed: 24390344]
46. Paulk NK, Pekrun K, Zhu E, Nygaard S, Li B, Xu J, Chu K, Leborgne C, Dane AP, Haft A, Zhang Y, Zhang F, Morton C, Valentine MB, Davidoff AM, Nathwani AC, Mingozzi F, Grompe M, Alexander IE, Lisowski L, Kay MA. Bioengineered AAV capsids with combined high human liver transduction in vivo and unique humoral seroreactivity. *Mol Ther.* 2017 in press.
47. Desnick RJ. Enzyme replacement and enhancement therapies for lysosomal diseases. *J Inherit Metab Dis.* 2004; 27:385–410. [PubMed: 15190196]
48. Amalfitano A, McVie-Wylie AJ, Hu H, Dawson TL, Raben N, Plotz P, Chen YT. Systemic correction of the muscle disorder glycogen storage disease type II after hepatic targeting of a modified adenovirus vector encoding human acid- α -glucosidase. *Proc Natl Acad Sci USA.* 1999; 96:8861–8866. [PubMed: 10430861]
49. van Til NP, Stok M, Aerts Kaya FSF, de Waard MC, Farahbakhshian E, Visser TP, Kroos MA, Jacobs EH, Willart MA, van der Wegen P, Scholte BJ, Lambrecht BN, Duncker DJ, van der Ploeg AT, Reuser AJJ, Versteegen MM, Wagemaker G. Lentiviral gene therapy of murine hematopoietic stem cells ameliorates the Pompe disease phenotype. *Blood.* 2010; 115:5329–5337. [PubMed: 20385789]
50. Manno CS, Chew AJ, Hutchison S, Larson PJ, Herzog RW, Arruda VR, Tai SJ, Ragni MV, Thompson A, Ozelo M, Couto LB, Leonard DGB, Johnson FA, McClelland A, Scallan C, Skarsgard E, Flake AW, Kay MA, High KA, Glader B. AAV-mediated factor IX gene transfer to skeletal muscle in patients with severe hemophilia B. *Blood.* 2003; 101:2963–2972. [PubMed: 12515715]
51. Mack DL, Poulard K, Goddard MA, Latournerie V, Snyder JM, Grange RW, Elverman MR, Denard J, Veron P, Buscara L, Le Bec C, Hogrel J-Y, Brezovec AG, Meng H, Yang L, Liu F, O’Callaghan M, Gopal N, Kelly VE, Smith BK, Strande JL, Mavilio F, Beggs AH, Mingozzi F, Lawlor MW, Buj-Bello A, Childers MK. Systemic AAV8-mediated gene therapy drives whole-body correction of myotubular myopathy in dogs. *Mol Ther.* 2017; 25:839–854. [PubMed: 28237839]
52. Ramos J, Chamberlain JS. Gene therapy for Duchenne muscular dystrophy. *Expert Opin Orphan Drugs.* 2015; 3:1255–1266. [PubMed: 26594599]
53. Raben N, Nagaraju K, Lee E, Kessler P, Byrne B, Lee L, LaMarca M, King C, Ward J, Sauer B, Plotz P. Targeted disruption of the acid α -glucosidase gene in mice causes an illness with critical features of both infantile and adult human glycogen storage disease type II. *J Biol Chem.* 1998; 273:19086–19092. [PubMed: 9668092]
54. Parenti G, Fecarotta S, la Marca G, Rossi B, Ascione S, Donati MA, Morandi LO, Ravaglia S, Pichiecchio A, Ombrone D, Sacchini M, Pasanisi MB, De Filippi P, Danesino C, Della Casa R, Romano A, Mollica C, Rosa M, Agovino T, Nusco E, Porto C, Andria G. A chaperone enhances blood α -glucosidase activity in Pompe disease patients treated with enzyme replacement therapy. *Mol Ther.* 2014; 22:2004–2012. [PubMed: 25052852]
55. Ruza A, Garcia M, Ribera A, Villacampa P, Haurigot V, Marcó S, Ayuso E, Anguela XM, Roca C, Agudo J, Ramos D, Ruberte J, Bosch F. Liver production of sulfamidase reverses peripheral and ameliorates CNS pathology in mucopolysaccharidosis IIIA mice. *Mol Ther.* 2012; 20:254–266. [PubMed: 22008915]
56. Gonzales PA, Pisitkun T, Hoffert JD, Tchapyjnikov D, Star RA, Kleta R, Wang NS, Knepper MA. Large-scale proteomics and phosphoproteomics of urinary exosomes. *J Am Soc Nephrol.* 2009; 20:363–379. [PubMed: 19056867]
57. Andrews NW. Regulated secretion of conventional lysosomes. *Trends Cell Biol.* 2000; 10:316–321. [PubMed: 10884683]

58. Sun B, Bird A, Young SP, Kishnani PS, Chen Y-T, Koeberl DD. Enhanced response to enzyme replacement therapy in Pompe disease after the induction of immune tolerance. *Am J Hum Genet.* 2007; 81:1042–1049. [PubMed: 17924344]
59. Sun B, Kulis MD, Young SP, Hobeika AC, Li S, Bird A, Zhang H, Li Y, Clay TM, Burks W, Kishnani PS, Koeberl DD. Immunomodulatory gene therapy prevents antibody formation and lethal hypersensitivity reactions in murine Pompe disease. *Mol Ther.* 2010; 18:353–360. [PubMed: 19690517]
60. Markusic DM, Hoffman BE, Perrin GQ, Nayak S, Wang X, LoDuca PA, High KA, Herzog RW. Effective gene therapy for haemophilic mice with pathogenic factor IX antibodies. *EMBO Mol Med.* 2013; 5:1698–1709. [PubMed: 24106230]
61. Crudele JM, Finn JD, Siner JI, Martin NB, Niemeyer GP, Zhou S, Mingozzi F, Lothrop CD Jr, Arruda VR. AAV liver expression of FIX-Padua prevents and eradicates FIX inhibitor without increasing thrombogenicity in hemophilia B dogs and mice. *Blood.* 2015; 125:1553–1561. [PubMed: 25568350]
62. Bortolussi G, Zentillin L, Vaníková J, Bockor L, Bellarosa C, Mancarella A, Vianello E, Tiribelli C, Giacca M, Vitek L, Muro AF. Life-long correction of hyperbilirubinemia with a neonatal liver-specific AAV-mediated gene transfer in a lethal mouse model of Crigler–Najjar Syndrome. *Hum Gene Ther.* 2014; 25:844–855. [PubMed: 25072305]
63. Meliani A, Boisgerault F, Ronzitti G, Collaud F, Leborgne C, Kishimoto TK, Mingozzi F. Antigen-specific modulation of capsid immunogenicity with tolerogenic nanoparticles results in successful AAV vector readministration. *Mol Ther.* 2016; 24:pS34.
64. Meliani A, Leborgne C, Triffault S, Jeanson-Leh L, Veron P, Mingozzi F. Determination of anti-adenovirus-associated virus vector neutralizing antibody titer with an in vitro reporter system. *Hum Gene Ther Methods.* 2015; 26:45–53. [PubMed: 25819687]
65. Ayuso E, Mingozzi F, Montane J, Leon X, Anguela XM, Haurigot V, Edmonson SA, Africa L, Zhou S, High KA, Bosch F, Wright JF. High AAV vector purity results in serotype- and tissue-independent enhancement of transduction efficiency. *Gene Ther.* 2010; 17:503–510. [PubMed: 19956269]
66. Masat E, Laforêt P, De Antonio M, Corre G, Perniconi B, Taouagh N, Mariampillai K, Amelin D, Mauhin W, Hogrel J-Y, Caillaud C, Ronzitti G, Puzzo F, Kuranda K, Colella P, Mallone R, Benveniste O, Mingozzi F. French Pompe Registry Study Group. Long-term exposure to Myozyme results in a decrease of anti-drug antibodies in late-onset Pompe disease patients. *Sci Rep.* 2016; 6:36182. [PubMed: 27812025]
67. Zhang P, Sun B, Osada T, Rodriguiz R, Yang XY, Luo X, Kemper AR, Clay TM, Koeberl DD. Immunodominant liver-specific expression suppresses transgene-directed immune responses in murine Pompe disease. *Hum Gene Ther.* 2012; 23:460–472. [PubMed: 22260439]
68. Moreland RJ, Jin X, Zhang XK, Decker RW, Albee KL, Lee KL, Cauthron RD, Brewer K, Edmunds T, Canfield WM. Lysosomal acid α -glucosidase consists of four different peptides processed from a single chain precursor. *J Biol Chem.* 2005; 280:6780–6791. [PubMed: 15520017]
69. Deming, DT. *Molecular Genetics and Metabolism.* Vol. 117. Elsevier; 2016. p. S14-S124.

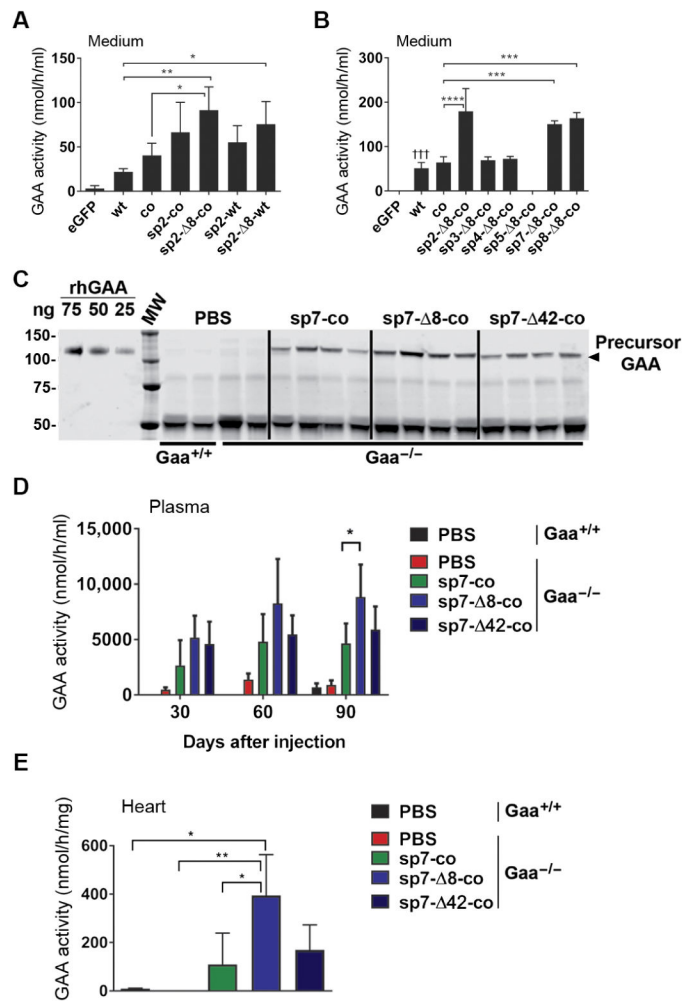


Fig. 1. Selection of engineered human GAA transgenes in vitro and in vivo

(A and B) Acid α -glucosidase (GAA) activity in conditioned media of HuH7 cells; enhanced green fluorescent protein (eGFP), negative control. Data are means \pm SD of three independent experiments. wt, wild-type human GAA transgene; co, codon-optimized human GAA transgene; sp, signal peptide; Δ , deleted human GAA. (C to E) In vivo testing of adeno-associated virus (AAV) vectors expressing secretable GAA. Four-month-old mice were treated with phosphate-buffered saline (PBS) or with 2×10^{12} vector genomes (vg)/kg of different AAV8 vectors and followed for 3 months. GAA transgenes were under the control of the hAAT promoter; Gaa^{+/+}-PBS ($n = 2$), wild-type littermates; Gaa^{-/-}-PBS ($n = 3$), untreated control; sp7-co ($n = 4$); sp7- Δ 8-co ($n = 4$); and sp7- Δ 42-co ($n = 4$). (C) Western blot analysis of plasma from treated mice, 3 months after treatment. The band detected at \sim 50 kDa in both PBS- and vector-treated Gaa^{-/-} mice is nonspecific. Recombinant human GAA (rhGAA) was used as standard. MW, molecular weight marker. (D) GAA activity in plasma at different times after injection and (E) heart. Statistical analysis: one-way analysis of variance (ANOVA) with Tukey's post hoc (A, B, and E) or two-way ANOVA (treatment, time) with Dunnett's post hoc (D). Error bars represent SD of the mean. In (B), $^{\dagger\dagger\dagger}P < 0.001$ compared to sp2- Δ 8-coGAA, sp7- Δ 8-coGAA, and sp8- Δ 8-coGAA.

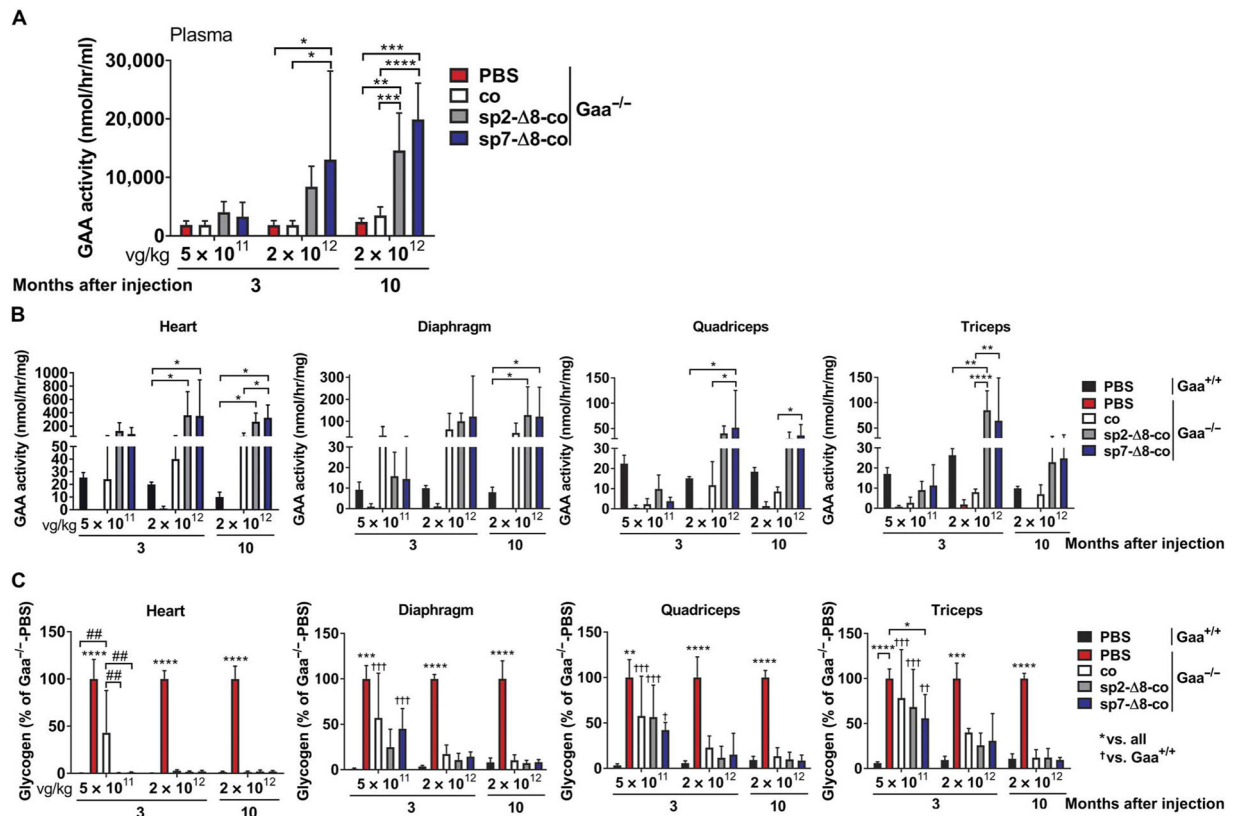


Fig. 2. GAA activity and tissue glycogen in vivo

(A to C) Four-month-old mice were treated with PBS or AAV8 at the vector doses indicated and followed for 3 months ($n = 4$ to 5 per cohort) or 10 months ($n = 8$ to 9 per cohort; $n = 3$ GAA^{-/-}-PBS cohort; GAA^{+/+}-PBS, wild-type littermates; GAA^{-/-}-PBS, untreated control). (A) GAA activity in plasma. (B) GAA activity in different muscles. (C) Glycogen content in different muscle reported as percentage of PBS-treated GAA^{-/-} mice. (A to C) Statistical analysis: two-way ANOVA with Tukey's post hoc (treatment, dose). Error bars represent SD of the mean. (C) Asterisks (*) indicate significant differences compared to all groups; dagger symbols (†) indicate significant differences compared to GAA^{+/+}-PBS. * or †, $P < 0.05$; ** or ††, $P < 0.01$; *** or †††, $P < 0.001$; **** or ††††, $P < 0.0001$.

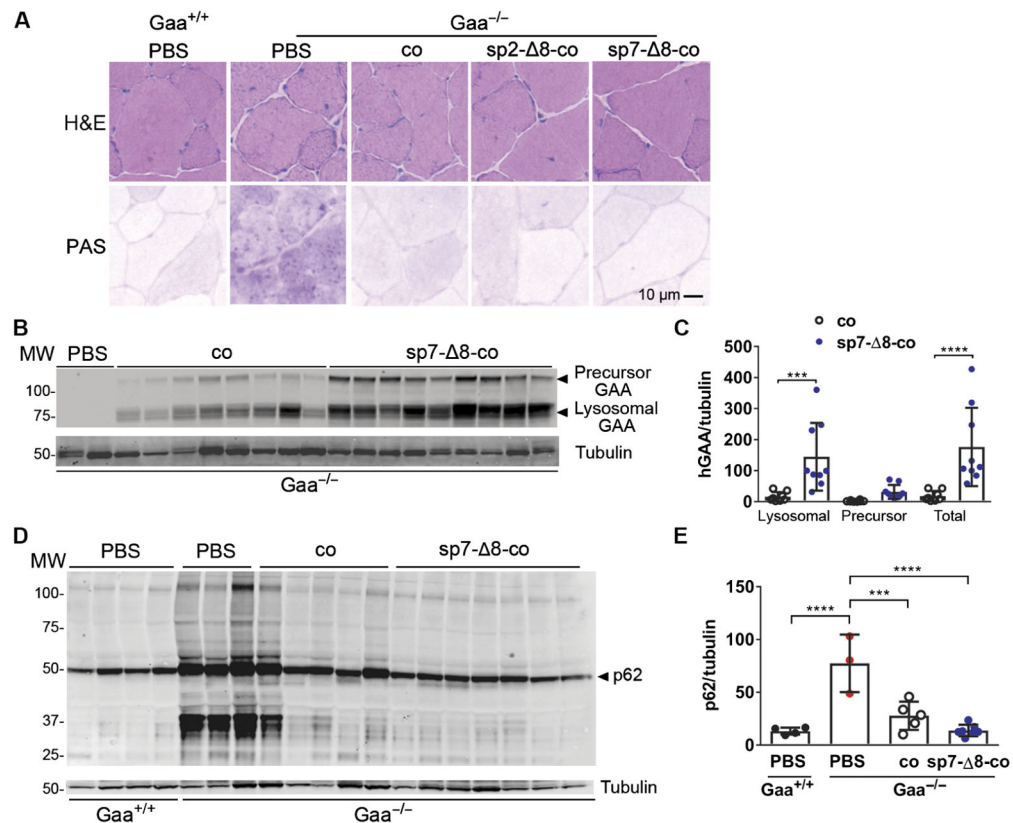


Fig. 3. Histology, GAA uptake, and autophagic buildup in triceps of treated *Gaa*^{-/-} mice and controls

(A to E) Analysis of triceps in mice 10 months after treatment with AAV8 (2×10^{12} vg/kg). *Gaa*^{+/+}-PBS, wild-type littermates; *Gaa*^{-/-}-PBS, untreated control. (A) Representative images of hematoxylin and eosin (H&E, top) and periodic acid-Schiff (PAS, bottom) staining of triceps. The scale bar is depicted. (B and D) Western blot analysis of triceps lysates using anti-GAA (B) or anti-p62 (D) monoclonal antibodies. An anti-tubulin antibody was used as loading control. (C and E) Quantification of GAA (C) or p62 (E) bands from the corresponding Western blots. Statistical analysis: (C) multiple *t* tests, with Sidak-Bonferroni post hoc. *Gaa*^{-/-}-PBS, *n* = 2; *Gaa*^{-/-}-co, *n* = 8; *Gaa*^{-/-}-sp7-8-co, *n* = 9. (E) One-way ANOVA with Tukey's post hoc. *Gaa*^{+/+}-PBS, *n* = 4; *Gaa*^{-/-}-PBS, *n* = 3; *Gaa*^{-/-}-co, *n* = 5; *Gaa*^{-/-}-sp7-8-co, *n* = 7. Error bars represent the SD of the mean.

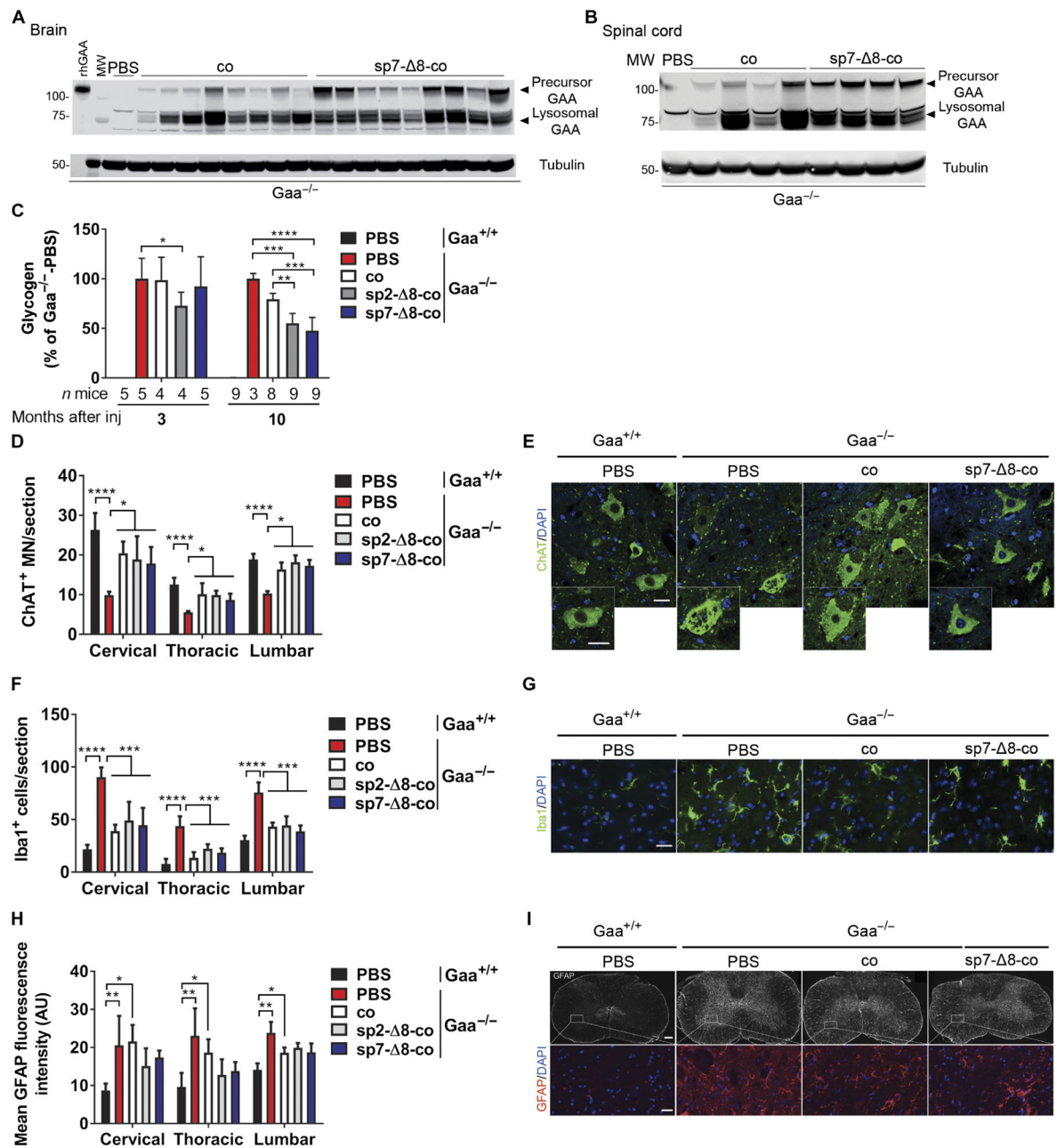


Fig. 4. Analysis of brain and spinal cord of treated $Gaa^{-/-}$ mice and controls

(A to I) Four-month-old mice treated with PBS or AAV8 vectors (2×10^{12} vg/kg) and followed for 3 months ($n = 4$ to 5 per cohort) or 10 months ($n = 8$ to 9 per cohort; $n = 3$ $Gaa^{-/-}$ -PBS). $Gaa^{+/+}$ -PBS, wild-type littermates; $Gaa^{-/-}$ -PBS, untreated control. Western blot analysis of brain (A) and cervical spinal cord (B) lysates 10 months after treatment using a monoclonal anti-GAA antibody. An anti-tubulin antibody was used as loading control. (C) Quantification of glycogen content in brain 3 and 10 months after treatment. The quantification is reported as percentage of glycogen in $Gaa^{-/-}$ mice treated with PBS. (D to I) Analysis of spinal cord 10 months after treatment. (D) Count of choline acetyl

transferase-positive (ChAT⁺) motor neurons (MN) in spinal cord. (E) Representative images of ChAT staining. (F) Count of ionized calcium binding adaptor molecule 1-positive (Iba1⁺) cells in the gray matter of spinal cord. (G) Representative images of Iba1 staining. (H) Glial fibrillary acidic protein (GFAP) fluorescence quantification in the gray matter of the spinal cord. AU, arbitrary units. (I) Representative images of GFAP staining. In all images, cells were stained with the nuclear marker 4',6-diamidino-2-phenylindole (DAPI). Scale bars, 200 μm (I, top) and 25 μm (E, G, and I, bottom). (D to I) *Gaa*^{-/-}-PBS, $n = 2$; $n = 3$ for the other cohorts. Error bars represent SD of the mean. Statistical analysis: (C) two-way ANOVA with Tukey's post hoc (treatment, time); (D, F, and H) two-way ANOVA with Tukey's post hoc (treatment, region of spinal cord).

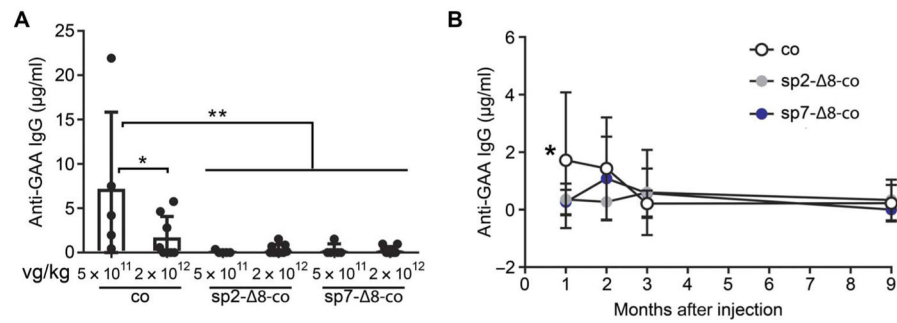


Fig. 5. Anti-human GAA humoral immune responses in $Gaa^{-/-}$ mice

(A and B) Analysis of anti-human GAA immunoglobulin G (IgG) in plasma samples from treated $Gaa^{-/-}$ mice. (A) Anti-human GAA IgG measured at 1 month after treatment at a vector dose of 5×10^{11} vg/kg ($n = 5$ per cohort) or 2×10^{12} vg/kg ($n = 8$ to 9 per cohort). (B) Anti-human GAA IgG over time in animals treated at a vector dose of 2×10^{12} vg/kg ($n = 8$ to 9 per cohort). Error bars represent the SD of the mean. Statistical analysis: (A) one-way ANOVA with Dunnett's post hoc; (B) two-way ANOVA with Tukey's post hoc (treatment, time). (B) * $P < 0.05$ for co at 1 month compared to sp2- 8-co or sp7- 8-co at 1 month, and co at 1 month compared to co at 3 or 9 months.

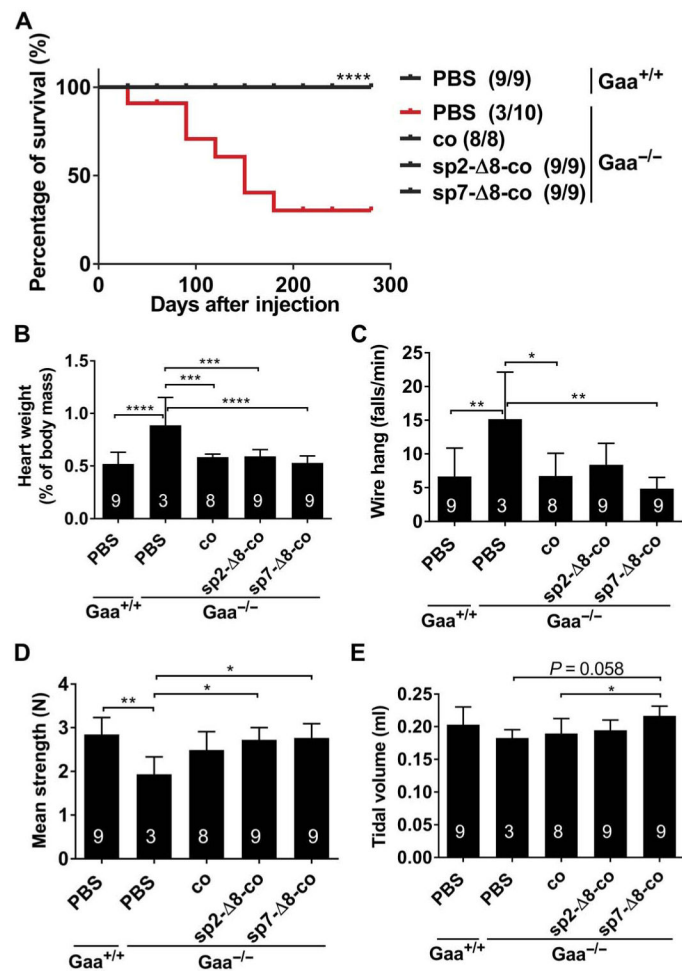


Fig. 6. Long-term outcome of gene therapy in treated $Gaa^{-/-}$ mice and controls (A to E) Four-month-old mice treated with PBS or AAV8 vectors (2×10^{12} vg/kg) and followed for 10 months ($n = 8$ to 9 per cohort; $n = 3$ $Gaa^{-/-}$ -PBS). $Gaa^{+/+}$ -PBS, wild-type littermates; $Gaa^{-/-}$ -PBS, untreated control. (A) Kaplan-Meier curve showing the percentage of survival from 4 to 14 months of age. The number of live animals per cohort at the end of the study is indicated in brackets. **** $P < 0.0001$ compared to $Gaa^{-/-}$ -PBS, log-rank Mantel-Cox test. (B) Cardiac hypertrophy showed as heart weight expressed as percentage of body mass. (C to E) Functional tests 9 months after treatment. (C) Wire hang test shown as falls per minute. (D) Grip test as mean of three independent measurements. (E) Tidal volume measured by whole-body plethysmography. Statistical analysis: one-way ANOVA with Tukey's post hoc (B to D) or Dunnett's post hoc (E). The number of animals per treatment cohort is shown in the histogram bars. Error bars represent the SD of the mean.

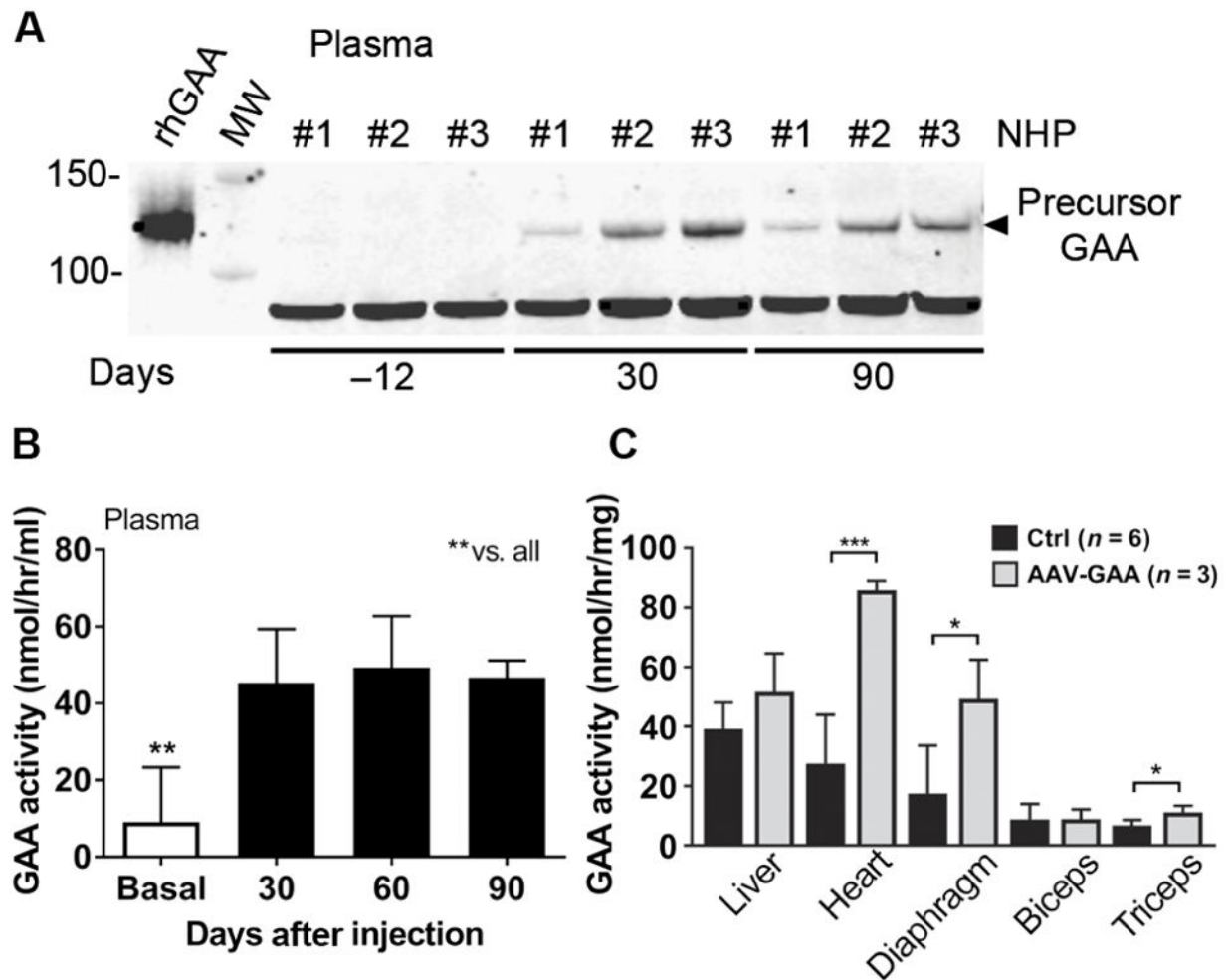


Fig. 7. Scale-up of AAV vector-mediated liver gene transfer of secretable GAA to nonhuman primates

(A to C) Male cynomolgus monkeys ($n = 3$) were treated with AAV8-hAAT-sp7-8-coGAA (AAV-GAA) (2×10^{12} vg/kg) and followed up for 90 days. (A) Western blot analysis of plasma using an anti-GAA antibody. rhGAA was used as loading control. NHP, nonhuman primate. (B) GAA activity in plasma. Basal, endogenous GAA activity in monkeys #1 to #3 before injection and five additional control monkeys ($n = 8$). Statistical analysis: one-way ANOVA with Tukey's post hoc. Error bars represent the SD of the mean. (C) GAA activity in liver, heart, diaphragm, biceps, and triceps. Endogenous GAA activity was measured in six monkeys treated with an unrelated AAV vector [control (Ctrl)]. Statistical analysis: multiple t test.

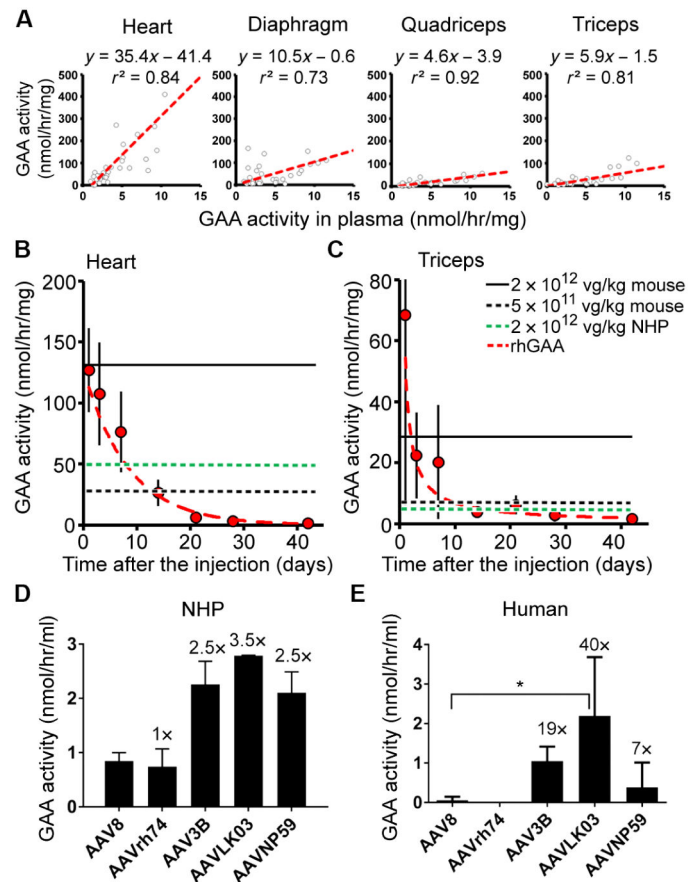


Fig. 8. Therapeutic potential of AAV vector-mediated liver gene transfer for Pompe disease
(A) Regression plots showing the correlation between GAA activity measured in plasma compared to heart, diaphragm, quadriceps, or triceps in AAV-*GAA*-treated *Gaa*^{-/-} mice. Combined data from 3 months in vivo experiments (tables S1 and S2). The linear regression formula and the regression coefficient (r^2) are depicted. **(B and C)** Time course of GAA activity in heart (B) and triceps (C) of *Gaa*^{-/-} mice infused with rhGAA at 100 mg/kg biweekly for a total of two infusions. Each time point represents the average of four to six animals. Error bars represent SD of the mean. Red lines, activity regression curves. Horizontal black lines mark the median GAA activity measured in tissues of *Gaa*^{-/-} mice 3 months after treatment with AAV8-hAAT-sp7-8-co*GAA* vectors at 2×10^{12} vg/kg (solid line) or 5×10^{11} vg/kg (dotted line). The horizontal green line indicates the mean (after baseline subtraction) GAA activity measured in tissues of monkeys 3 months after treatment with the same AAV8-hAAT-sp7-8-co*GAA* vector at a dose of 2×10^{12} vg/kg. **(D and E)** GAA activity measured in the conditioned media of primary NHP (D) or human (E) hepatocytes 48 hours after transduction with different serotypes of AAV-hAAT-sp7-8-co*GAA* vector at a multiplicity of infection of 1×10^5 . The numbers above the bars indicate the fold increase of GAA activity compared to AAV8-transduced cells. Means of two-well testing for (D) are shown. Error bars in (E) represent the SD of the mean of three independent experiments except for AAVrh74 ($n = 1$). Statistical analysis: one-way ANOVA with Dunnett's post hoc.